Control Strategy for Optimum Utilization of Self-Excited Induction Generator Connected to a Public Network

Saeed A. Al-Ghamdi

Electric Eng. Dept., Faculty of Engineering, Albaha University, Al-Baha, KSA
Emails: sasg2000@gmail.com

Abstract: This paper investigates a new control strategy of a wind energy driven by a variable speed wind turbine self-excited induction generator (SEIG) connected to a public network. Also, the steady state analysis of the SEIG is introduces taking the saturation effects into consideration. The proposed system consists of a three-phase induction generator feeds its stator electrical output power into an infinite bus-bar via a static power conditioner. The power conditioner used here consists of a diode bridge rectifier and an inverter bridge thyristor tied together through a d.c. link reactor of high inductance. The SEIG in this work driven by a variable speed wind turbine is proposed with a fixed pitch angle to reduce the system cost and easy to run.At higher generator speeds, the generated voltage as well as the stator current exceeds its rated values resulting in generator thermal overheating. At low wind speeds the SEIG operates at constant generated voltage, increasing the wind speed increases the generated power which results increasing of the stator current. In order to protect the generator against this thermal overheating, the generator should be controlled via the power conditioner to maintain rated stator current. So, it becomes necessary to add two loops in order to automatically control and protect the generator. The first loop operates in the speed range under the rated stator current to keep the generator voltage constant at rated value. As soon as the stator current attains its rated value, the second control loop automatically controls the system to run at constant rated stator current to obtain optimum generator utilization without overheating. The obtained theoretical and experimental steady state characteristics demonstrate effectiveness of the proposed strategy.
[Saeed A. Al-Ghamdi. **Control Strategy for Optimum Utilization of Self-Excited Induction Generator Connected to a Public Network.** *J Am Sci* 2014;10(7):19-28]. (ISSN: 1545-1003). http://www.jofamericanscience.org. 5

Key Words: Wind turbine, Induction generator, Static power conditioner, Public network, Voltage control, Current control, Interface circuit, and Toggle switch.

1. Introduction

In recent years, due to the increasing prices and depletion of conventional energy sources, interest in renewable energy resources such as wind and solar has intensified. Also, the fossil fuel, gas and coal result in air pollution and increase the call for that clean energy sources. The increasing energy demand throughout the world, the air pollution produced by fossil fuel as well as the limited reserves of this fuel and the growing doubt about the safety of nuclear power led to a growing demand for the wider use of renewable energy sources such as wind. Wind energy has the advantages that, it is clean and inexhaustible. Various schemes for generating electricity from wind have been proposed. One of these schemes is the SEIG connected to an infinite bus-bar using rectifier – dc link – inverter scheme in the stator circuit which is the subject of this paper. It is widely known that an induction machine can self-excite when a suitable capacitance is connected across its stator terminals and the rotor is driven by a prime-mover. Under such conditions, the terminal capacitance furnishes the lagging reactive power necessary for establishing the air gap flux. This phenomenon is termed the "capacitor self-excitation", which can be exploited to operate the induction machine as a generator. The induced voltages and currents would continue to rise, but for magnetic saturation in the machine which results in an equilibrium state being reached and the machine is often referred to a SEIG [1-4].

Because of the gust structure of the wind, and because of a cyclical variation in the turbine-blade loading caused by tower shadow and wind shear, severe mechanical and electrical stresses can be induced in the generator. Consequently, a rare or compliant damped coupling is usually interposed between the synchronous generator and the wind turbine. **Johnson and Smith** [5] suggested that, the use of an induction generator could be obviate the need for such coupling. **El-Sadek et al** [6] developed a control system for on-line simulation of wind turbine by separately excited d.c. motor and the SEIG performance with isolated load is derived. The wind electric energy conversion systems (WEECS) are

classified based upon the type of turbine (fixed or variable pitch turbine) and the electric generator type. Constant speed is often obtained by using variable pitch turbines and the fixed turbines usually produce a variable speed [7]. An attempt has been made to present a simple model to control the output voltage and frequency in case of SEIG under varying wind speeds operation [8]. **Nassereddine et al [9],** showed the advantages of using a Switched Reluctance Generator (SRG) for wind energy applications. The theoretical study of the self-excitation of a SRG and the determination of the variable parameters in a SRG design are discussed.

The control is to be accomplished electrically by adjusting the inverter firing advance angle β. The steady state analysis of a wind energy driven (SEIG) connected to an unified supply network taking the saturation effect into consideration investigated in El-Lithy, et al., & Hasaneen and Nada [10, 11]. The steady state analysis and performance of a SEIG driven by regulated and unregulated turbines is discussed by **Chan** [12]. The influence of both of rotor resistance and excitation capacitor on the steady state performance characteristics of a wind energy driven SEIG is studied in El-Lithy, [13].

Nada and Al-Ghamdi [14] has been investigated an analytical approach for matching the characteristics of a fixed pitch angle wind turbine with that of a SEIG. The wind turbine's performance curve, power coefficient versus tip speed ratio, is represented by a polynomial function of both the generator speed and the wind speed. At any given generator speed the wind turbine output mechanical power is equated to the SEIG input mechanical power. From this mechanical power balance a non-linear equation for the wind speed is resulted. **Deraz and Abdel Kader** [15] has been presented a new control strategy of a stand-alone self-excited induction generator (SEIG) driven by a variable speed wind turbine. The proposed system is modeled and simulated using Matlab/Simulink software program to examine the dynamic characteristics of the system with proposed control strategy.

The steady state analysis carried out in this paper is based on presents the effect of variation of saturation on the system performance. The machine magnetizing inductance varies considerably owing to saturation. The effect of this variation will be taken into account in this paper. Here, the same terminal capacitor needed for self-excitation determined used in the following calculations. In the mathematical model presented here, the average effect of the static power conditioner-a.c. network combination is replaced by an equivalent variable resistance. A steady state mathematical model for the system under load conditions is derived and the whole system characteristics are obtained.

The energy conversion scheme in this work has no synchronizer and doesn't need pitch angle control. Accordingly, the absence of these devices reduces the weight of the turbine generator system which must be located on the top of the wind turbine tower. Hence, it is simple, easy to run, and cheap.

2. System Description and Analysis Considering Saturation

Figure 1 shows the single line diagram of the system under study with different constituting parts. A diode bridge rectifier is preferably used to achieve an operation of the induction generator always at nearly unity power factor. The rectified direct current is smoothed by a reactor of high inductance acting as an intermediate circuit to decouple the machine and the inverter with a.c. supply network.

The analysis here is carried out with the following assumptions:

i- The direct current is assumed to be completely smoothed and ripple free.

ii- Only the fundamental components are considered.

iii- Commutation in inverter bridge is ignored (the valves are assumed to be ideal switches).

iv- Only the magnetizing reactance is assumed to be affected by magnetic saturation (taking variation of saturation into consideration).

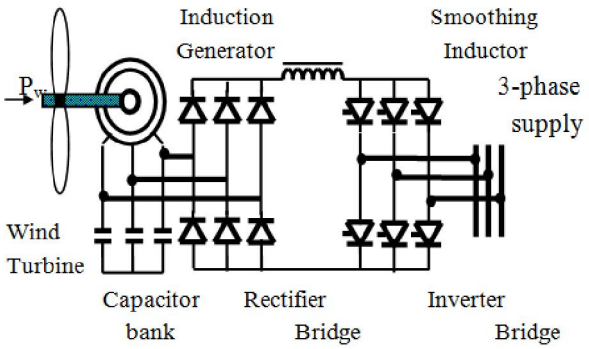

Fig. 1: Single line diagram of the system.

For an induction generator to be self-excited, the machine has to operate in the saturation region [16,17]. Therefore, for a given speed and load, the terminal capacitor should have a value such that the magnetizing reactance always lies in the saturated region. Let X_m be the maximum saturated magnetizing reactance of the machine, which can be experimentally determined [11]. Even though, the X_{ms} of the machine

varies considerably with operating conditions (owing to saturation).

2.1 Equivalent Resistance of the Static Power Conditioner and A.C. Network

The action of static power conditioner - a.c. network combination on the average is replaced by an equivalent variable resistance. This resistance is designated R_L/F and is connected across the stator terminals [13]. Combining this resistance with the SEIG steady state equivalent circuit we obtain a complete equivalent circuit describing the steady state behaviour of the SEIG - static power conditioner - a.c. network combination as shown in Fig. 2. This figure represented the per phase steady state equivalent circuit of SEIG with resistive load across its stator terminals considering variation of saturation.

The equivalent resistance R_L /F determines the active power transferred from the generator to the a.c. network across the static power conditioner. The equation describing R_L/F in terms of the network a.c. voltage V_n, the load current I_L, the inverter firing advance angle , the direct current I_d in the d.c. link reactor, and the generator terminal voltage V_g can be estimated by equating the power in this resistance with the active power transferred to the a.c. network.

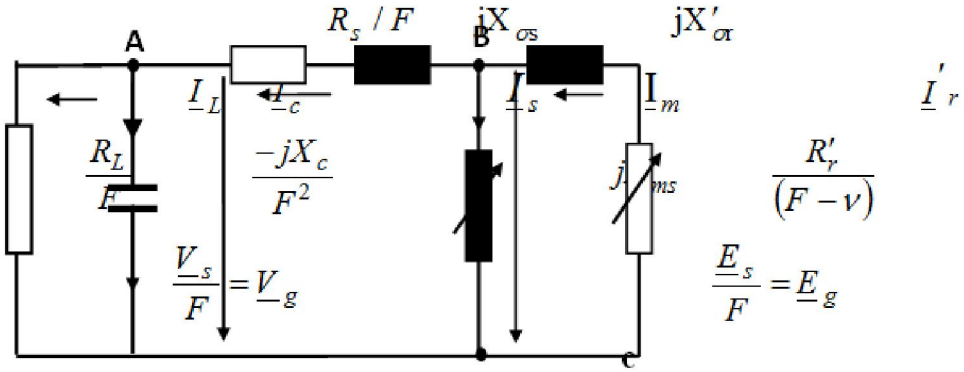

Fig. 2: Equivalent circuit of the SEIG of the system.

Referring to Ref. [13] and the equivalent circuit of Fig. 2 we can write:

$$3\,I_L^2\left(\frac{R_L}{F}\right) = \frac{3\sqrt{6}}{\pi} V_n \cos(\beta).I_d \quad (1)$$

As before the d.c. current I_d and the fundamental r.m.s. load current I_L are related together by the following relation [18-20]:

$$I_d = \frac{\pi}{\sqrt{6}} I_L \quad (2)$$

Substitution of Eq. (2) into Eq. (1) yields:

$$\frac{R_L}{F} = \frac{V_g}{I_L} = \frac{V_n}{I_L}\cos(\beta) \quad (3)$$

2.2 Determination of Self Excitation Frequency under Load

The relationship determining the per unit self-excitation frequency F under load for a certain value of saturated magnetizing reactance X_{ms} can be derived from the mesh equation for the stator current I_s from Fig. 2 [16]. Thus:

$$Z_t \underline{I}_s = 0 \quad (4)$$

where Z_t is the net loop impedance. This impedance is equal to:

$$Z_t = Z_{AC} + Z_{AB} + Z_{BC} \quad (5)$$

The different impedance's of the above equation are:

$$Z_{AC} = \frac{\frac{-jX_c}{F^2}\cdot\frac{R_L}{F}}{\frac{R_L}{F} - \frac{jX_c}{F^2}} \quad (6a)$$

$$Z_{AB} = \frac{R_s}{F} + jX_{\sigma s} \quad (6b)$$

$$Z_{BC} = \frac{jX_{ms}\cdot\left[\frac{R'_r}{F-\nu} + jX'_{\sigma r}\right]}{\frac{R'_r}{F-\nu} + jX'_{\sigma r} + jX_{ms}} \quad (6c)$$

And:

Since under steady state conditions for successful voltage build-up, $I_s \neq 0$, it follows from Eq. (4) that, $Z_t = 0$. This implies that, the real and imaginary parts of Z_t each equals zero. Separate the real and imaginary parts of Z_t to zero yields the following two relations for the load resistance R_L / F.

$$\frac{R_L}{F} = \frac{-\frac{X_c}{F^2}\cdot\left[X'_r\cdot\frac{R_s}{F} + X_s\cdot\frac{R'_r}{F-\nu}\right]}{\frac{X_c}{F^2}.X'_r - \left[K - \frac{R_s}{F}\cdot\frac{R'_r}{F-\nu}\right]} \quad (7a)$$

$$\frac{R_L}{F} = \frac{\frac{X_c}{F^2}\cdot\left[K - \frac{R_s}{F}\cdot\frac{R'_r}{F-\nu}\right]}{\frac{X_c}{F^2}\cdot\frac{R'_r}{F-\nu} - \left[X'_r\cdot\frac{R_s}{F} + X_s\cdot\frac{R'_r}{F-\nu}\right]} \quad (7b)$$

And:

where: $K = X_{os}.X'_r + X'_{or}.X_{ms}$, (8a)

$X_s = X_{os} + X_{ms}$, (8b)

$X'_r = X'_{or} + X_{ms}$ (8c)

Since the value of R_L/F must satisfy both Eq. (7a) and Eq. (7b) simultaneously, the right hand sides of these equations should be equated and by algebraic manipulations the following 4th degree polynomial in the per unit self-excitation frequency F is obtained:

$$C_1F^4 + C_2F^3 + C_3F^2 + C_4F + C_5 = 0 \quad (9)$$

The nameplate data and parameters of the induction generator under study are given in Appendix A1 and the detailed expressions describing these coefficients (C_1 : C_5) are given in Appendix A2. For a given operating speed and a certain value of X_{ms}, Eq. (9) is solved numerically using Newton-Raphson method to obtain the per unit self-excitation frequency F.

2.3 Performance Equations

To determine the magnetizing reactance at different induced air gap voltage E_g, the machine was supplied from the a.c. supply (no-load test), and the input impedance per phase was measured at different input voltages. As we need the variation of X_{ms} with the air gap flux, proportional to E_g, it is necessary to calculate the air gap induced voltage by subtracting the voltage drop in the stator leakage impedance from the input voltage. Figure 3 shows the experimental results relating X_{ms} with E_g. The variation of X_{ms} with E_g will be nonlinear due to magnetic saturation. In the analysis presented here curve fitting is used to obtain a mathematical expression for the curve X_{ms} -E_g. This relation is obtained to:

$$X_{ms} = K_1 + K_2E_g + K_3E_g^2 \text{ (p.u.)} \quad (10)$$

The constants K_1, K_2 and K_3 depend on the design and material of the machine. Here, these constants are found to be:

$K_1 = 2.0269$, $K_2 = 0.7507$, and $K_3 = -1.5373$ (11)

This relation can be incorporated in the computer program. By assuming the induced air gap voltage E_g, the per unit saturated magnetizing reactance X_{ms} can be calculated from Eq. (10). Then the per unit self-excitation frequency F can be computed from Eq. (9) for any value of speed.

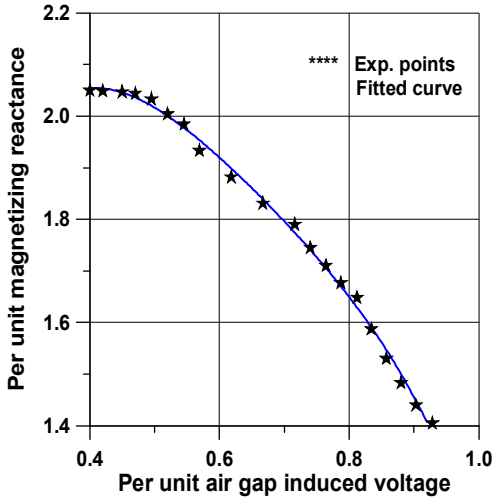

Fig. 3: P. U. magnetizing reactance versus P. U. air gap induced voltage.

Knowing E_g, X_{ms}, F, X_c, and the other machine parameters from Appendix A1, calculation of the terminal voltage V_g and the generator currents can be determined using the equivalent circuit of Fig. 2. Firstly, the magnetizing current is calculated from:

$$\underline{I}_m = \frac{\underline{E}_g}{jX_{ms}} \quad (12)$$

The referred rotor current $\underline{I}'_r$ is obtained to:

$$\underline{I}'_r = \frac{\underline{E}_g}{R'_r/(F-\nu) + jX'_{or}} \quad (13)$$

The stator current can be determined as:

$$\underline{I}_s = \underline{I}'_r - \underline{I}_m \quad (14)$$

Then, the terminal generator voltage V_g is:

$$\underline{V}_g = \underline{E}_g - \underline{I}_s\left(\frac{R_s}{F} + jX_{os}\right) \quad (15)$$

The capacitor current $\underline{I}_c$ and the load current $\underline{I}_L$ are computed from:

$$\underline{I}_c = \frac{\underline{V}_g}{-jX_c/F^2} \quad (16)$$

and: $\underline{I}_L = \underline{I}_s - \underline{I}_c$ (17)

The relation between the direct current in the intermediate d.c. circuit and the load current is given by Eq. (2).

Having determined the currents, the active power transferred to the a.c. network, the total copper losses

(stator and rotor) and consequently the input mechanical power as well as the efficiency can be easily deduced. The active power transferred to the a.c. network from the stator terminals through the static power conditioner is obtained as:

$$P_g = 3\,\text{Real}\left\{\underline{V}_g.\underline{I}_L^*\right\} = 3\frac{\sqrt{6}}{\pi}V_n\cos(\beta).I_d \quad (18)$$

The total copper losses are computed from:

$$P_{cu} = P_{cs} + P_{cr} = 3.\left(R_s I_s^2 + R'_r I'^2_r\right) \quad (19)$$

The addition of Eqs. (18) and (19) yields the input internal mechanical power; thus:

$$P_m = P_g + P_{cu} \quad (20)$$

Once the input and output active power relations are computed, the generator efficiency can be determined from:

$$_g = P_g / P_m \quad (21)$$

3. Control Concept of the SEIG

When the generator is controlled to operate at constant voltage, the stator current rises as the speed rises [11]. Accordingly, there is a certain operating speed above which the stator current exceeds its rated value resulting in generator thermal overheating. In order to protect the generator against this overheating the machine should be controlle power conditioner to maintain rated stator current. Consequently, in order to obtain optimum ger utilization without thermal overheating, the generator should be operated as possible with X_{ms} and controlled via the oner to operate under the following control strategy:

To the control circuit (3)

Interface Circuit

Error Amplifier

i -In the speed r ıich the stator current is lower than its rated value (at low wind speed) the generated voltage must be kept constant at this rated value by maintaining the inverter control angle β at its minimum permissible value.

ii- As soon as the stator current attains its rated value the inverter control angle β is adjusted (increased) to maintain this current all over the remainder operating range at rated value.

3.1 Voltage Control Loop

In order to realize optimum utilization for the SEIG, the generated voltage should be kept constant at its maximum permissible value during the first operating range. This range begins from the no-load speed till the stator current attains its rated value. The voltage control loop operates in this range, while. the current control loop is completely blocked to allow the current to increase with the speed. The proposed system with the two control loops and toggle switch are schematically shown in Fig 4.

The firing angle automatic adjustment system consists of an interface circuit and an error amplifier as shown in Fig. 5. This voltage sensing circuit is labeled by number **1** in Fig. 4.

Interface circuits, are used to rescale the DC link voltage to a proper voltage level that drives the error amplifier. They are configured as a lumped resistor that insures an accurate and safe operation of the amplifier.

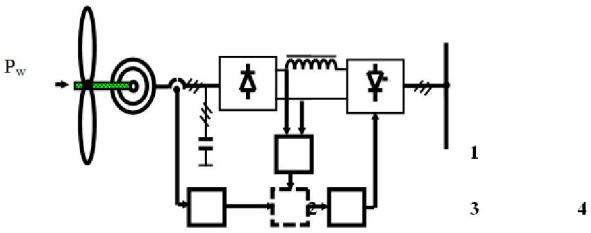

Fig. 4: Single line diagram of the system.
1 d.c. link measurement,
2 stator current measurement,
3 electronic toggle switch,
4 control devices.

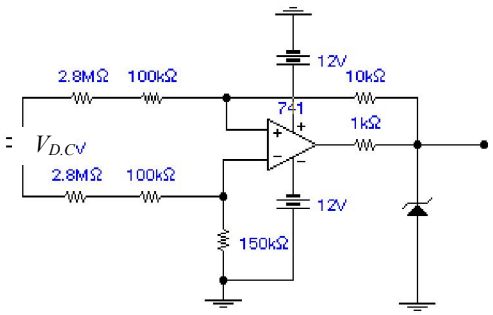

Fig. 5: A simple circuit for a voltage attenuator of the d.c. link.

Error amplifier, is an important stage by which controlling the firing angle of the inverter is performed. The two inputs of the error amplifier are the rescaled voltage of the DC link and a predetermined reference voltage labled by number **1** in Fig. 4. The reference voltage is designed based on the maximum available voltage of the SEIG. The amplifier output error voltage is then compared with a triangle waveform to provide a proper switching angle of the inverter labled by number **4** in Fig. 4.

3.2 Current Control Loop

The wind-electric energy conversion in a wider speed range is more reliable than the conversion in a limited range. Then, one can think about increasing the range in which the wind energy can be injected to the public network. As mentioned before, operation at constant generator voltage results in an increased stator current by increasing the wind speed. So, we

must limit this current at its rated value in order to avoid overheating the generator windings. Increasing the range of the wind-electric energy conversion using such topology can be fulfilled by compensating the increased of the stator current. This current can be kept constant by controlling the firing advance angle of the inverter bridge. However, limiting the stator current results in a reduction of the injected power to the public grid. One can therefore predict an increasing of the efficiency of the whole wind-electric energy converter.

The current controller should be designed for rated generator stator current. The proposed loop is labeled by number **2** in Fig. 4. The current limiting circuit consists of **Transformer, Full-wave single-phase bridge rectifier and Voltage amplifier**.

For interfacing the generator current, we must sense an alternating voltage proportional to the generator stator current. For this reason, we insert three equal small resistors (0.2 ohm) in the three phase stator winding. The primary of the voltage transformer (step up transformer) is connected in shunt with one of these resistors to measure the stator current. The voltage across that resistor results in an induced voltage at the secondary terminal of the transformer. One can consider a linear proportionality between the induced voltage and the stator current, a single-phase full-wave bridge rectifier is used for rectifying the induced secondary voltage of the transformer and then used to determine the switching instants of the inverter. A diagram for the stator current limiting circuit is shown in Fig. 6.

The limiting stator current loop extends the dynamic range of the wind-electric converter. However, this current loop reduces the injected power to the public utility network as the wind speed increases. In this range the voltage control loop is completely blocked, but the current control loop is in operation. Furthermore, the stator current limiting loop is complementary working with the loop of controlling the terminal generator voltage.

3.3 Toggle Switch

The system is capable to work probably with either extending the dynamic range mode (stator winding protection) or with the stabilization of DC link voltage mode (controlling the terminal generator voltage). It has also the advantage of increased reliability where it is automatically switching between the two mode mentioned above.

An analog switch (4066) is used as **a toggle switch** to either connect the stabilization voltage mode or connect the extending dynamic range loop to the gate drive circuit of the current link inverter. At low speeds the first loop is in action until the stator current attains its rated value, at this time, the toggle switch is automatically switching the controller to work with the second loop. Also, the toggle switch is capable to switch automatically the controller from the second loop to the first loop depending on the stator current. The control circuit of the system (toggle switch) is shown in Fig. 7. This toggle switch is labeled by number **3** in Fig. 4. The proposed circuit is evaluated and laboratory tested.

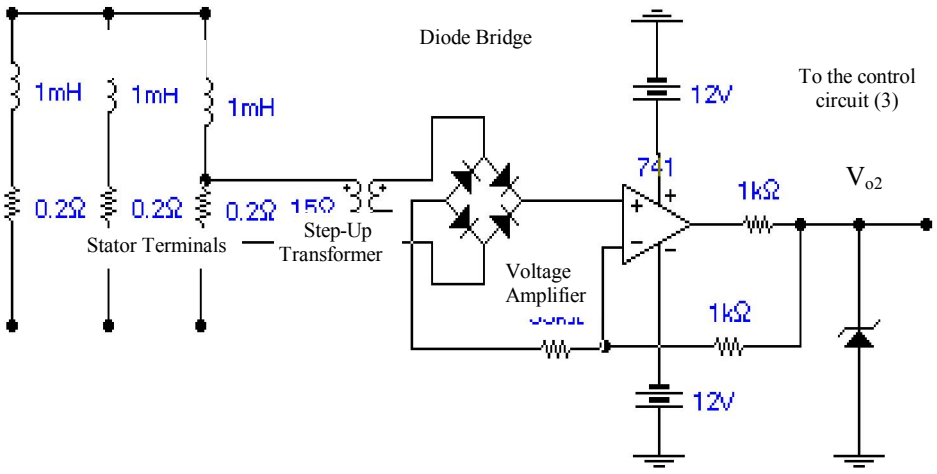

Fig. 6: The circuit for limiting the generator stator current.

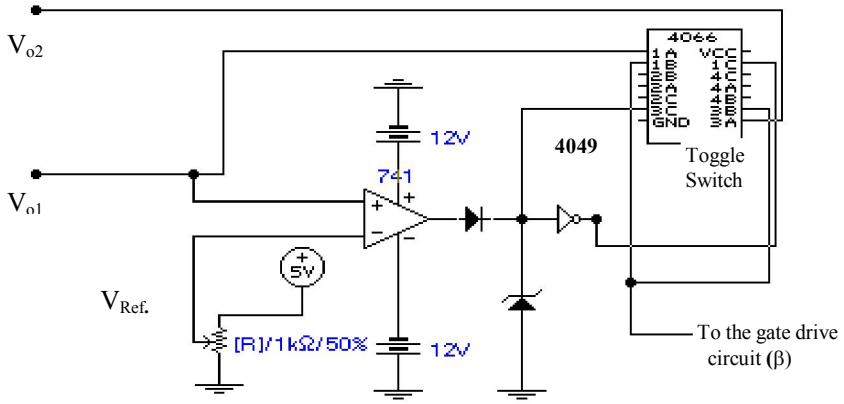

Fig. 7: The Control circuit of the system (toggle switch).

4. Theoretical and Experimental Results

Some difficulties found in the laboratory such as the insufficient current rating of the converter transformer and the armature voltage rating of the d.c. motor prevent the experimental work to be carried out at the induction machine rated voltage and current. All tests have been carried out using a three phase capacitor bank for self excitation C = 70 μF which is available in the laboratory.

The experimental work is carried out with constant generated voltage at 0.35 p.u and constant stator current at 0.5 p.u. With the proposed two loops to automatically adjust the inverter firing advance angle β, the system can be operated at any wind speed values without any risk. So, the proposed circuits are evaluated and laboratory tested with the whole system.

The automatically adjusted inverter firing advance angle β versus the per unit speed is shown in Fig. 8. The control angle β at the constant generated voltage mode is kept approximately constant at minimum value. As soon as the stator current attains half its rated value (test maximum value) the toggle switch drive the current control loop to keep the stator current constant at this value. In this mode the control angle β increases as the speed rises to reduce the generated voltage, in order to maintain the stator current at its maximum predetermined value. As shown in this figure, there is a good agreement between the experimental and the computed results.

Steady state characteristics with automatic control strategy versus per unit speed are shown in the figures 9, 10, 11 and 12. These figures show the obtained experimental results of the operation parameters compared with the corresponding obtained theoretical results. Theoretical (computed) results is continuous lines —, and the experimental results are stars ****.

It is clear that the experimental results are very close to the computed results. This confirms that the two control loops automatically adjust the inverter firing advance angle β are operating satisfactorily. Also, the transition from the constant voltage mode to the constant stator current mode is evident. This means that the toggle switch is automatically switching the controller from the constant voltage mode to the constant stator current mode. When the system operates on the constant generated voltage mode, the stator current as well as the direct current increase with the speed. So, the generated power increases as the speed rises. But, when the system operates on the constant stator current mode, the generated voltage decreases and consequently the generated power.

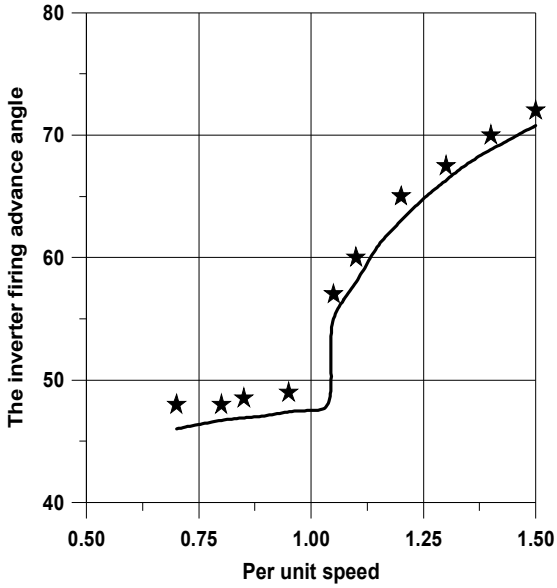

Fig 8: Inverter firing advance angle versus per unit speed.

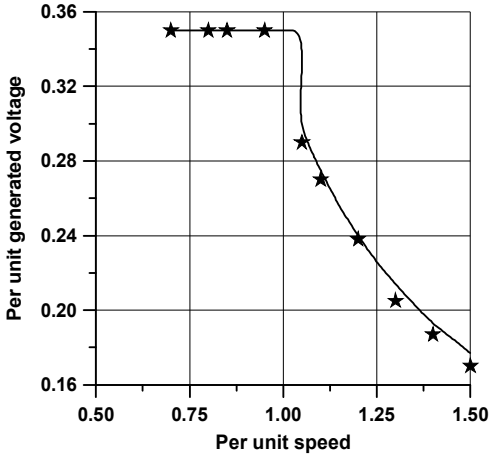

Fig 9: Generated voltage

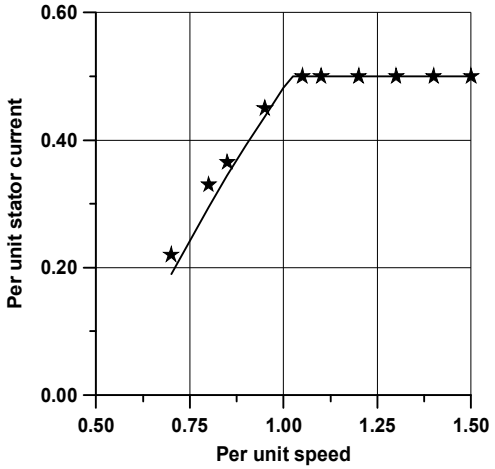

Fig 10: Stator current.

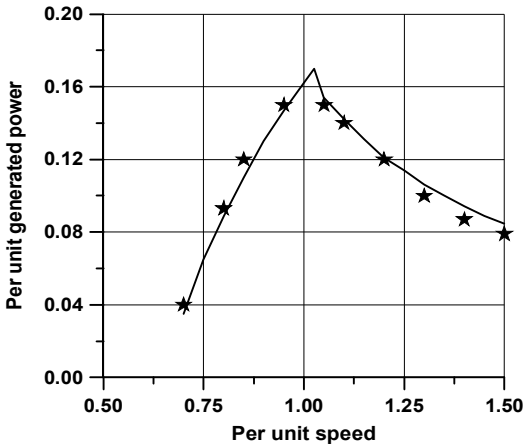

Fig 11: Generated power.

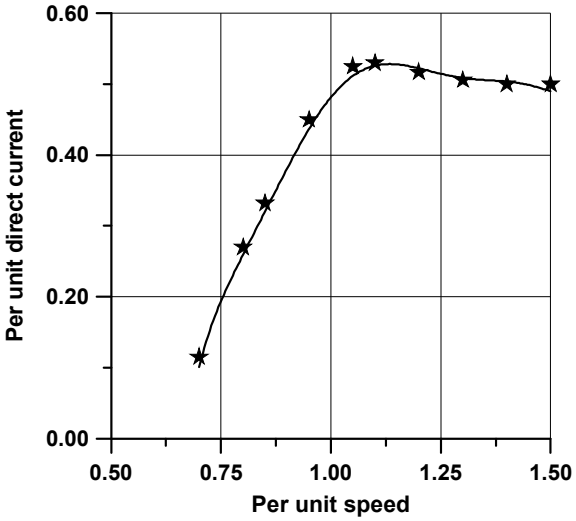

Fig 12: Direct current.

5. Conclusions

It is important to mention that for stable operation of SEIG, the machine has to operate in the saturation region. Therefore, for a given speed, the excitation capacitor should have a value such that the machine magnetizing inductance always lies in the saturation region. On the other hand the machine magnetizing inductance varies considerably owing to saturation. So, a more accurate analysis is carried out considering the variation of saturation is presented. In this analysis determining the frequency of self-excitation under load is very easy to calculate from very simple equation.

The adding two loops in order to automatically control and protect the generator from overheating is necessary. The first loop operates in the speed range under the rated stator current to keep the generator voltage constant. As soon as the stator current attains its rated value, the second control loop automatically controls the system to run at constant rated stator current using the toggle switch.

This energy conversion scheme of SEIG has no synchronizer and doesn't need pitch angle control. Accordingly, the absence of these devices reduces the weight of the turbine generator system which must be located on the top of the wind turbine tower. Hence, it is simple, easy to run, and cheap.

References

1. Atallah, M. Ahmed. “Terminal Voltage Control of Self Excited Induction Generators”, Sixth Middle-East Systems Conference (MEPCON’ 98), Mansoura, Egypt, Dec. 1998, pp. 110-118.
2. Shaltout, A.A. and Abdel-Halim, M.A. “Solid State Control of a Wind Driven Self Excited Induction Generator”, Electric Machines and Power Systems, 23: 571-582, 1995.
3. Chan, T.F. “Steady State Analysis of Self Excited Induction Generators”, IEEE Trans. on Energy Conversion, Vol. 9, No. 2, June 1994, pp. 288-296.
4. Murthy, S.S., Sing, B.P., Nagamani, C. and Satyanarayana, K.V.V. “Studies on the Use of Conventional Induction Motors as Self Excited Induction generators”, IEEE Trans. on Energy Conversion, Vol. 3, No. 4, Dec. 1988, pp. 842-848.
5. Johnson, C.C. and Smith, R. T. Dynamic of wind generators on electric utility networks, IEEE trans., Vol. AES-12, No. 4, July 1976, pp. 483-493.
6. El-Sadek, M.Z., Saady, G. and Abdel-Mohsen, T.: “On-Line Simulation of Wind Turbine by Separately Excited DC Motor Driving Self Excited Induction Generator”, Sixth Meddle-East Systems Conference (MEPCON’ 98), Mansoura, Egypt, Dec. 1998, pp. 105-109.
7. Salameh, Z.M., and Kazda. “A design Method for Matching the Characteristics of a Double Output Induction Generator (DOIG) with the Performance Characteristics of Wind Turbines”, Proc. of the Midwest Power Conference, Nov. 1982, pp. 1-10.
8. Sandhu, K.S. and Jain, S.P. “Steady State Operation of Self-Excited Induction Generator with Varying Wind Speeds”, International Journal of Circuits, System and Signal Processing, Issue, Vol. 2, 2008, pp. 26-33.
9. Nassereddine, M., Rizk, J. and Nagrial, M. “Switching Reluctance Generator for Wind Power Applications”, World Academy of science, Engineering and Technology, 41, 2008, pp. 126-130.
10. El-Lithy F.M., A. S. Nada and M. A. Elwany. "A Wind Driven Self-Excited Reluctance Generator Steady-State Operating Limits", Al Azhar University Engineering Journal (AUEJ), Vol. 8, No. 10, April, 2005, pp. 68-77.
11. Hasaneen M. and A. S. Nada. "Performance Analysis of a Self-Excited Induction Generator at Constant Stator Current Considering Saturation", 11th International Middle East Power System Conference, IEEE-MEPCON 2006, Egtypt, Menia University, Vol. 1, Dec. 2006, pp. 399-405.
12. Chan, T.F. “Self Excited Induction Generators Driven by Regulated and Unregulated Turbines”, IEEE Trans. on Energy Conversion, Vol. 11, No. 2, June 1996, pp. 338-343.
13. El-Lithy, F.M. “Influence of the Rotor Resistance and Excitation Capacitor on the Performance of a Wind Driven Self Excited Induction Generator”, Ain-Shams University, Faculty of Eng., Scientific Bulletin, Vol. 30, No. 3, Sept. 1995, pp. 102-117.
14. Nada A.S., and Saeed A. Al-Ghamdi. "Matching a Wind Turbine with a Self-Excited Induction Generator", Journal of American Science 2013; 9 (6), pp. 607-614.
15. Deraz S.A. and F.E. Abdel Kader. "A new control strategy for a stand-alone self-excited induction generator driven by a variable speed wind turbine", Renewable Energy, Vol. 51, 2013, pp. 263-273.
16. Say, M.G. “Alternating Current Machines”, Fourth Edition, London, Pitman (ELBS) 1976.
17. Fitzgerald, Kingsley and S. D. Umans. "Electrical Machinery", McGraw Hill, New-York, 2003.
18. Lander, W. “Power Electronics”, McGraw Hill, London, 1981.
19. Muhammad H. Rashid. “Power Electronics Circuits, Devices and Application”, Third Edition, Prentice-Hall, Englewood Cliffs, New Jersey, 2004.
20. Grade Frey Boyle. “Renewable Energy”, Second Edition, London, Pitman 2000.

Appendices

A1: The nameplate data and parameters of the induction generator under study are:

1.8 kW, 1400 r.p.m, 4-pole, 50 Hz, 220/380 V (Δ/Y), and 7.8/4.5 A (Δ/Y).

R_s = 2.22 Ω, R'_r = 3.1 Ω, $X_{\sigma s}$ = 5.0 Ω,

$X'_{\sigma r}$ = 5.0 Ω, X_m = 99.5 Ω.

The Base Values are: Base current, $I_b = I_{sn}$ = 4.5 A, Base Voltage, $V_b = V_n$ = 220 V

Base Power, $P_b = P_n$ = 2970 W.

A2: Coefficients C_1 - C_5 Introduced in Eq. (9)

$C_1 = K^2$, $C_2 = -2 \nu K_6$,

$C_3 = \nu^2 K_6 + 2 X_m^2 M_4 - X_c M_3 + M_1 + M_2$

$C_4 = 2\nu M_3 X_c - 2\nu M_4 X_m^2 - 2\nu M_1$,

$C_5 = \nu^2 M_1 + M^2_4 - M_5 X_c - \nu^2 M_3 X_c$

With: $M_1 = R_s^2 X_r'^2$, $M_2 = R_r'^2 X_s^2$,

$M_3 = K X'_r$, $M_4 = R_s R'_r$, and $M_5 = X_s R_r'^2$

And: $X_s = X_{\sigma s} + X_m$, $X'_r = X'_{\sigma r} + X_m$

5/6/2014